

# UCLA

## UCLA Previously Published Works

### Title

Acetylene Adsorption on Pd-Ag Alloys: Evidence for Limited Island Formation and Strong Reverse Segregation from Monte Carlo Simulations

### Permalink

<https://escholarship.org/uc/item/1zr3077q>

### Journal

JOURNAL OF PHYSICAL CHEMISTRY C, 122(27)

### ISSN

1932-7447

### Authors

Vignola, Emanuele  
Steinmann, Stephan N  
Le Mapihan, Katell  
et al.

### Publication Date

2018

### DOI

10.1021/acs.jpcc.8b04108

Peer reviewed

# Acetylene Adsorption on Pd-Ag Alloys: Evidence for Limited Island-Formation and Strong Reverse Segregation from Monte Carlo Simulations

Emanuele Vignola,<sup>†‡</sup> Stephan N. Steinmann,<sup>†</sup> \* Katell Le Mapihan,<sup>§</sup> Bart D. Vandegehuchte,<sup>§</sup> Daniel Curulla<sup>§</sup> and Philippe Sautet<sup>†&¶\*</sup>

<sup>†</sup>Univ Lyon, ENS de Lyon, CNRS, Université Lyon 1, Laboratoire de Chimie UMR 5182, F-69342, Lyon, France

<sup>‡</sup>Total Research and Technology Gonfreville, BP 27, F-76700 Harfleur, France

<sup>§</sup>Total Research and Technology Feluy, Zone Industrielle Feluy C, Seneffe, Belgium

<sup>&</sup>Department of Chemical and Biomolecular Engineering, University of California, Los Angeles, Los Angeles, CA 90095, United States

<sup>¶</sup>Department of Chemistry and Biochemistry, University of California, Los Angeles, Los Angeles, CA 90095, United States

\*e-mail: Stephan.steinmann@ens-lyon.fr; sautet@ucla.edu; tel.: +33-4-72-72-81-55; 1-310-825-8485

---

**ABSTRACT:** Restructuring of alloy surfaces induced by strongly bound adsorbates is a well-established phenomenon occurring in catalysis and membrane science. In catalytic processes this restructuring can have profound effects since it alters the ensemble distribution between the as-prepared state of the catalyst and the catalytic surface under operando conditions. This work assesses the restructuring of Pd-Ag alloys induced by adsorption of acetylene in the framework of the ensemble formalism. A detailed Ising-type model Hamiltonian of the (111) surface plane is fitted to extensive Density Functional Theory computations. The equilibrium distributions under a realistic environment are then evaluated by a Monte Carlo approach as a function of temperature and alloy composition. Acetylene induces a strong reverse segregation within the relevant range of temperature. Therefore, the surface of Pd-Ag catalysts is almost entirely covered by Pd for bulk ratios  $< 0.8$  Ag/Pd, which is, in general, detrimental to the selectivity of Pd-Ag catalysts. Despite the very strong vertical segregation, acetylene only induces marginal in-plane ordering, i.e., the surface triangular ensembles follow random distributions as a function of the surface layer Ag-fraction quite closely. This can be explained by two factors: first, triangular sites are not sufficient to fully capture the diversity of acetylene binding energies on Pd-Ag alloy surfaces. Rather, an extended environment including the first coordination sphere is necessary, and leads to an overlap in terms of binding energy between weakly binding Pd<sub>3</sub> ensembles and strongly binding Pd<sub>2</sub>Ag ensembles. The second critical aspect is related to lateral interactions, which preclude adsorption of acetylene molecules on nearest neighbor triangular sites. Therefore, in a Pd<sub>3</sub> island, roughly two thirds of Pd<sub>3</sub> sites would be lost. Our study suggests that the equilibrium structure of these alloy catalysts under operando conditions are far from the state targeted by catalyst design, revealing a nearly unavoidable reason for loss of selectivity of the catalyst with time of operation.

---

## Introduction

Achieving novel properties by mixing of different substances is at the heart of chemistry. Solid solutions are particularly versatile for modifying condensed-phase properties, for example impurities can enhance the hardness of metals. The effect of carbon or trace metals on steel properties<sup>1</sup>

and the entropic hardening in highly-disordered materials,<sup>2,3</sup> are perhaps the best known examples. The thermodynamic description of alloys, as described in phase diagrams, allows to predict the evolution of a two-component solid system with macroscopic constraints, and thus to forecast defects in materials, assess thermal stability and segregation.

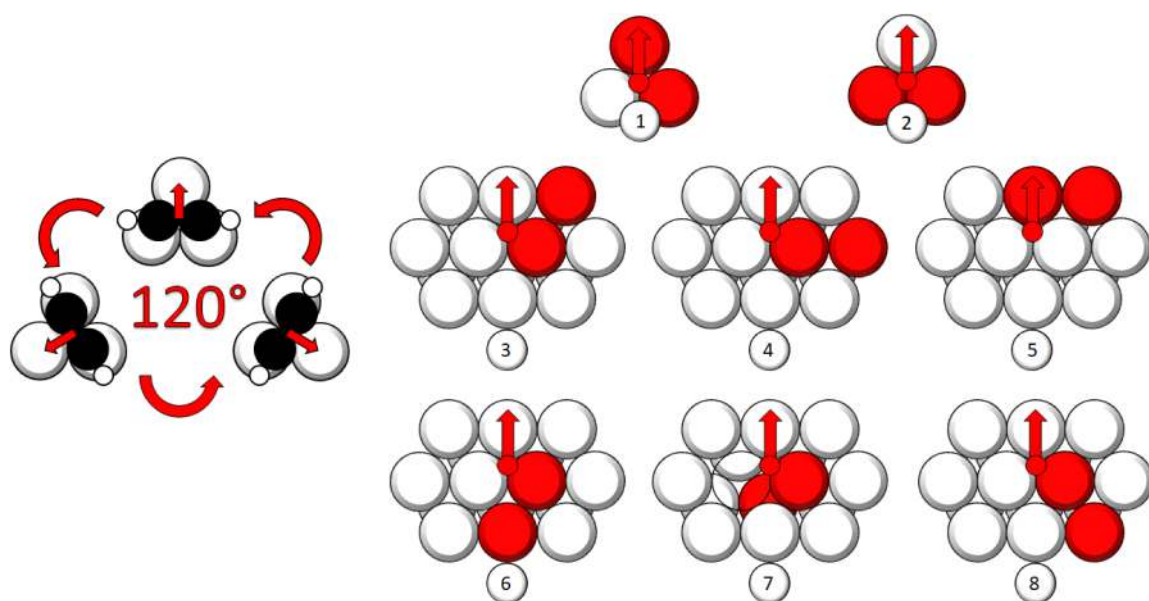


Figure 1. The effect of acetylene adsorption on pair interactions at the surface hollow site. Red atoms stand for atoms included in the cluster, white atoms for sites excluded. The red arrow is perpendicular to the C-C bond of acetylene, thus pointing toward the “weakly” interacting atom in the metal site (see text for more explanations).

Since catalysis and membrane science are particularly sensitive to surface phenomena, mastering alloy restructuring effects at surfaces is key. In this respect, building reliable models of the system’s energetics is essential as shown before.<sup>4</sup> Let us consider, for instance, the study of Pt-Pd nano-alloys by De Clercq and Mottet.<sup>5</sup> Here, a tight-binding, semi-empirical potential was fitted to DFT data and provided as input to a Monte Carlo algorithm. Along with the prediction of the segregation profile, decorations of onion-shell structures were explored as a function of particle size and of temperature. Apart from detailed insight on the alloy structure, this study was vital to understand changes in catalyst performance which is driven by surface effects.<sup>6</sup> A full comprehension of these phenomena can only be achieved by accounting for adsorbate-catalyst interactions in the model Hamiltonian. It is nowadays clear that environmental factors may significantly alter the compositional profile of the alloy topmost layers, especially if they are in contact with a gaseous reservoir, a typical situation in catalysis.<sup>7</sup> For instance, when atoms and molecules adsorb preferentially on one component, the segregation profile can be reversed compared to vacuum conditions, where surface energies of the pure metal dominate. For example, some of us showed before that the adsorption of unsaturated aldehydes on the PtFe(111) surface induces the segregation of Fe towards the surface.<sup>8</sup> This is also the case of CO adsorption on the (100) plane of Pd-Au alloys, where competition between metal-adsorbate adsorption energy and adsorbate-adsorbate lateral

interactions generate stripes of Pd at room temperature.<sup>9</sup> An analogous example has been provided in the computational study of Chen *et al.*,<sup>10</sup> which highlights the effect of oxygen binding on Au-Ag on pattern formation. In the latter two mentioned studies, the energy was modelled by Ising-type Hamiltonians fitted to DFT calculations. Indeed, Ising-type Hamiltonians are extremely efficient to deal with large unit cells of alloys that do not undergo severe geometric rearrangements and are dominated by rather short-ranged interatomic interactions. Another remarkable case in this sense is the restructuring of Pd-Ag alloys for the selective hydrogenation of acetylene to ethylene. Extensive research has shown<sup>11-13</sup> that the presence of adsorbates on the catalytic surface reverts the composition at the gas-metal interface compared to vacuum. It is found that the Pd enrichment under a reactive atmosphere is detrimental for the selectivity of the catalyst.<sup>6,14</sup> This phenomenon was also investigated along the two directions parallel to the surface. The topmost layer of the alloy (111) plane has been described in terms of triangular *ensembles*,<sup>15</sup> i.e., arrangements of three metal atoms. In high vacuum conditions, STM measurements found that the ensembles (Pd<sub>3</sub>, Pd<sub>2</sub>Ag, PdAg<sub>2</sub> and Ag<sub>3</sub>) are randomly distributed for a wide span of conditions.<sup>16</sup> This finding was attributed to the small difference between Pd-Pd, Pd-Ag and Ag-Ag pair interactions. Our recent study<sup>17</sup> revealed that adsorption of acetylene modifies the ensemble distributions. In particular, island formation was predicted for layers close to chemical purity, i.e. with an Ag fraction either close to 0 or 1, while

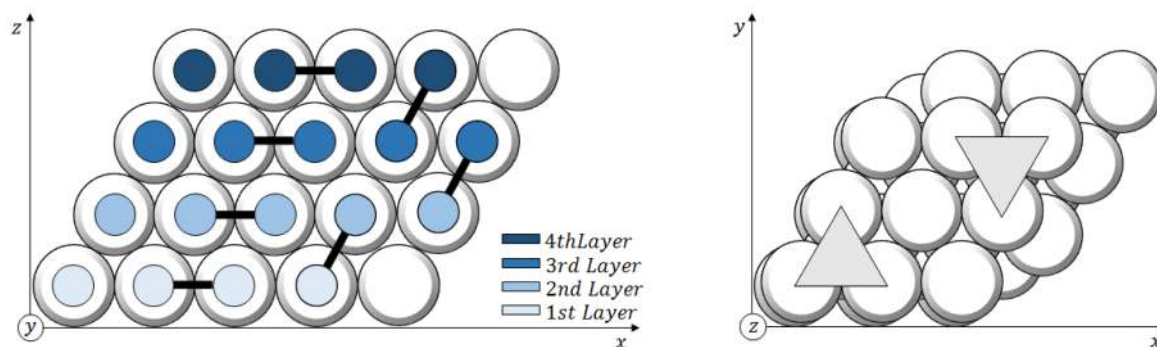


Figure 2. Catalyst model and selected interactions. Triangles in the top view (right part of the picture) denotes acetylene adsorption sites.

mixed ensembles prevail for equimolar ratios. These results were explained by the layer energy/entropy balance: the entropically driven random distributions are counterbalanced by the adsorption energy of acetylene which is much stronger on pure Pd than on mixed Ag-Pd ensembles. However, in that study the complexity of the system required rather strong approximations, among which a mean-field like treatment of lateral interactions and a local interpretation of the acetylene-ensemble bonding. Additionally, vertical segregation was completely neglected and interactions between molecules were assumed to be independent of the surface ensemble on which the acetylene molecule is adsorbed.

In order to overcome these limitations of the previous study and give an atomistic view on the surface state under realistic conditions, this paper describes the surface restructuring of Pd-Ag using a model Hamiltonian based on DFT calculations and integrated in a Monte Carlo code. Ensemble distributions are then computed as a function of temperature and alloy composition.

### Computational Details

All configurations were fully optimized at the Density Functional level of theory in the PAW formalism.<sup>18,19</sup> The computations were performed with VASP 5.3.3.<sup>20,21</sup> The functional of Perdew, Burke, and Ernzerhof<sup>22</sup> was used, with the dispersion correction of Steinmann and Corminboeuf.<sup>23</sup> The (111) surface was modelled by a  $p(3 \times 3)$  unit cell with 4 metallic layers, 2 of which were held fixed to simulate bulk properties. A vacuum layer of 15 Å was used and the lattice parameter determined according to Vegard's law, based on the optimized values at the PBE-dDsC level of theory for bulk Pd and Ag, which correspond to nearest neighbor distances of 2.78 and 2.92 Å, respectively. The plane waves basis set was chosen to have a cutoff energy of 400 eV. Brillouin zone integration was performed by a  $3 \times 3 \times 1$

Monkhorst-Pack<sup>24</sup> k-points grid and a Methfessel and Paxton<sup>25</sup> smearing of 0.2 eV. The wavefunction and geometric gradient were converged to  $10^{-6}$  eV and  $5 \times 10^{-2}$  eV/Å, respectively.

Numerical simulations were performed with an in-house FORTRAN90 Monte Carlo code provided in the SI. The code is based on repetitions of a 4-layers,  $p(2 \times 2)$  cell through real space. The number of repetitions is left as an input parameter. The user can choose the simulation temperature and the acetylene reservoir pressure, along with the Ag molar fraction of the 4 layers and the number of iterations. The system is then initialized to a random configuration. The configuration sampling is based on the Metropolis algorithm.<sup>26</sup> The chemical potential of the gaseous reservoir in the ideal gas approximation is calculated from statistical mechanics,<sup>27</sup> where the partition sum includes translational and rotational contributions (vibrational and electronic degrees of freedom are neglected). The output files provide ensemble distributions, their coverage, and the accepted geometries.

### *Ab initio* computations, construction of the model Hamiltonian and its validation

In order to access large unit cells and being able to equilibrate the ensemble distribution, we chose to model the system with an Ising-type Hamiltonian represented on a cluster basis.<sup>28</sup> Such a model requires a lattice of points distributed through the three dimensions of space. Each point in the lattice may be occupied by a Pd or an Ag atom. A specific chemical realization of the lattice is called a *configuration* of the system. For our purposes, the most important function of the system's configuration is the *configurational energy*. In the present work, the configurational energy is expanded in terms of two-body cluster contributions relative to atoms and adsorption sites. Ising-type Hamiltonians of alloys are analogous to the spin

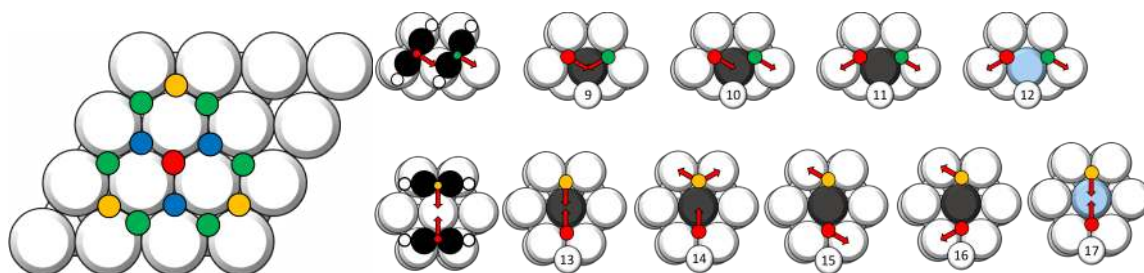


Figure 3. Lateral interactions parametrized in the model Hamiltonian. Red: Central adsorption site; dark blue: 1<sup>st</sup> nearest neighbour; green: 2<sup>nd</sup> nearest neighbour; yellow: 3<sup>rd</sup> nearest neighbour. The red arrow indicates the orientation of acetylene with respect to the triangular site (see also Figure 1). Grey and light blue represent Pd and Ag atoms, respectively. White atoms stand for sites not included in the cluster

Hamiltonians employed to model magnetic phenomena, but with one severe difference. As it is known, spins not only interact with each other, but also with an external field to which they can align to. Prediction of alloy phase diagrams does not require any contact with external fields. Nevertheless, a mathematical equivalence between external fields and gaseous reservoirs has been demonstrated.<sup>29</sup> This equivalence is of essence in the present context, although it must undergo some rewriting, due to the heterogeneity of acetylene adsorption. In fact, the acetylenic “field” will be described by an additional 2D gas-lattice layer superimposed to the lattice of metallic atoms. The local orientation of the acetylenic field relative to an adsorption site will be depicted with an arrow, as shown in Figure 1.

An aspect common to alloy systems is that the energy of a particular metallic species depends on its position with respect to the catalyst surface.<sup>30</sup> As a result, at equilibrium, one of the species (Pd or Ag) is expected to segregate at the surface. Distinct energy coefficients were therefore assigned to Pd and Ag atoms for each of the positions in the 4 layers. This is depicted in Figure 2, where interactions between nearest neighbors are also displayed. Due to linear dependencies between single and two-body clusters, we only included pair interactions in the model. Third-order and higher coefficients were neglected based on previous knowledge of the system.<sup>16</sup> Notice that both intra- and inter-layer contributions were considered in agreement with the symmetry loss along the normal axis ( $z$  axis of Figure 2). The number of metallic atom interaction terms to be included into the model amounts, therefore, to 24. These coefficients have been fitted on a set of 226 configurations of the bare surfaces.

To assess the effect of acetylene on the (111) surface plane of Pd-Ag alloys, the geometry of adsorption on palladium must be considered in the

first place. It is known<sup>31</sup> that acetylene adsorbs on palladium (111) at triangular hollow sites (see Figure 1 and 2). At low pressure and temperature, a molecule of acetylene lies in the middle of such sites, and the geometry of this di- $\sigma$  mode suggests that the molecule is strongly bound to two of the site’s atoms and weakly to the third one. The molecule seldom jumps to another site via a diffusional transition state where it interacts with two of the site’s metallic atoms – the so-called “bridge” mode. An additional local minimum is the  $\pi$  mode, where acetylene sits on only one metallic atom. Since triangles of 3 metallic atoms are enough to capture acetylene adsorption, surface-acetylene interactions are effectively described in terms of triangular ensembles. These triangular ensembles are reported in Figure 1, which also shows an important characteristic of the di- $\sigma$  mode: the site accommodates the molecule in three different orientations, generated by rotations of 120°. For the case of pure metal ensembles, *i.e.* Pd<sub>3</sub> and Ag<sub>3</sub>, the three rotations are degenerate in energy because of symmetry considerations. However, for the mixed ensembles, Pd<sub>2</sub>Ag and PdAg<sub>2</sub>, the site symmetry is lower, requiring the distinction between “weakly” and “strongly” interacting atoms. In other words, acetylene exhibits different orientations, as represented by an arrow normal to the C-C axis on Figure 1, pointing to the weakly interacting metal atom. The two kinds of atom (weakly and strongly interacting) may be either palladium or silver. This makes 7 energy coefficients describing the isolated acetylene adsorption with the triangular site in the model Hamiltonian. However, when considering various configurations of the Pd/Ag alloy, we found that the triangular model is oversimplified. Indeed, in order to have a reasonably accurate fit for the low coverage adsorption of acetylene, an extended environment has to be considered: on the surface, the complete set of nearest neighbours of the “strong” pair has to be included. Furthermore, the



2<sup>nd</sup> layer atoms close to the adsorption site (1 or 2 for fcc and hcp, respectively) also influence the adsorption energy. Interestingly, the central sub-surface atom (i.e., the one below the hcp site) does not play any role. To parametrize this extended environment, 24 more coefficients are required. The 31 two body interaction terms for the single adsorption mode of acetylene have been fitted to 150 configurations.

The 55 coefficients considered up to this point describe the adsorption process of an ideal lattice-gas adsorbed layer. As we have shown previously,<sup>17</sup> acetylene molecules adsorbed on Pd-Ag catalyst exert rather strong interactions between each other at short intermolecular distances. These lateral interactions must, therefore, be included in the model as well. Lateral interactions of nearest neighbor pairs (red to blue points in Figure 3) are found to be unphysical and are, therefore, excluded in the model Hamiltonian. Second (red to green) and third (red to yellow) nearest neighbor interactions were identified for various relative orientations (see Figure 3). Orientations not covered by the model Hamiltonian correspond to arrangements that do not exist on the relaxed DFT potential energy surface.

As displayed in Figure 3, lateral interactions are parametrized by a further set of 9 three-body terms. These parameters were fitted to 52 configurations with varying surface coverage and silver/palladium content. Hence, in total the model Hamiltonian contains 64 terms, fitted to a set of 428 DFT computations.

The fitting was done in three separate steps, one for the pure catalyst, one for the low coverage adsorption of acetylene and, finally, one for the lateral interactions. The numerical values were obtained by a least-squares fit, exploiting the Moore-Penrose pseudoinversion<sup>32</sup> of the following equation

$$\mathbf{E}_{DFT} = \mathbf{A} \cdot \boldsymbol{\epsilon} \quad (1)$$

Here,  $\mathbf{A}$  is a  $c \times p$  matrix whose elements are the occurrences of cluster in a given configuration,  $\mathbf{E}_{DFT}$  the  $1 \times c$  column vector of the  $c$  configuration total energies, and  $\boldsymbol{\epsilon}$  is the  $1 \times p$  column vector of  $p$  the cluster coefficients, also called parameters. We have checked that Cook's distances are below  $4/c$  as suggested by Bollen and Jackman,<sup>33</sup> so that all parameters are statistically well defined. Additionally, we have computed the uncertainties in the model parameters. As shown in Table S1 to S3, except for the lateral interactions, all parameters have low uncertainties. Furthermore, the values are chemically rather reasonable. Regarding the pure

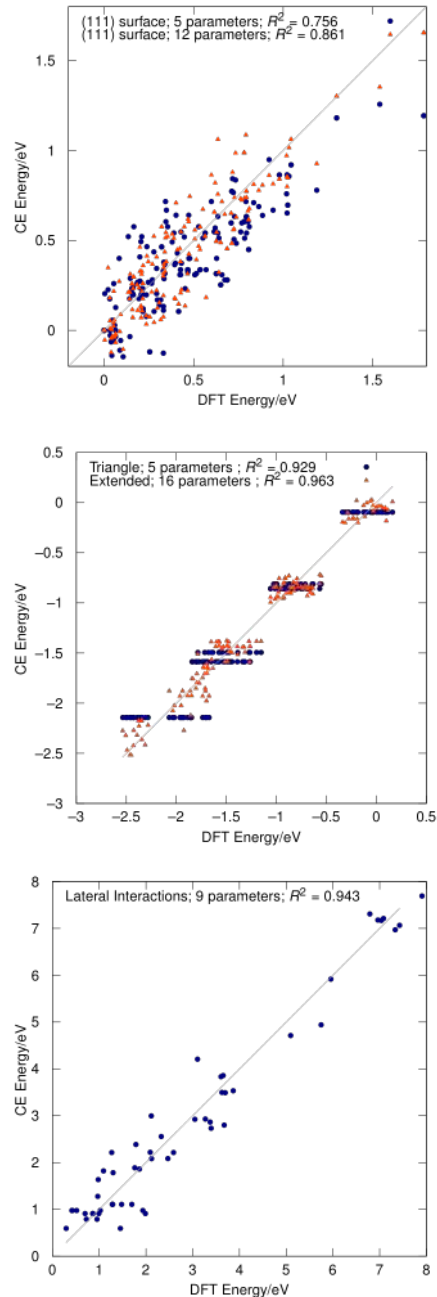


Figure 4. Parity plots of atomic swaps in bare surface models (top) and adsorption energies of a single acetylene molecule on various PdAg alloy surfaces (middle). Total lateral interactions for systems with 3 to 8 acetylene molecules on a  $p(4 \times 4)$  surface are given in the bottom graph. The number of independent variables is given in the legend.

surface, the major surprise is that the segregation is not visible in the Ag-Ag vs Pd-Pd coefficients as a function of the position in the layer. Nevertheless, the numerical simulations (vide infra) clearly show the expected segregation of Ag to the surface in the absence of acetylene adsorption, i.e., at high temperatures. We have found that the model Hamiltonian slightly overestimates the tendency of

mixing Pd with Ag on the surface, so that mixed ensembles are more probable than in a perfectly random alloy (see SI). However, extensive tests have shown that this tendency is so small that it has no visible influence on the obtained results. Coefficients associated to adsorption on Pd all favor the process, while interaction of acetylene with Ag is of little importance. The weak/strong relation between acetylene and metallic atoms is captured for Pd, with an energy difference between the two coefficients of 0.09 eV. In an analogous way, the coefficient of a weakly interacting Ag atom is 0.07 eV higher in energy than the strongly bonded one.

While least-squares interpolations are potentially subjected to overfitting,<sup>34</sup> i.e. not only do they model relevant information, but noise as well, our parity plots (Figure 4) clearly show that the complexity of our systems is larger than the (effective) number of parameters used to describe them. By effective parameters, we mean the rank of the occurrence matrix, i.e., the number of linearly independent variables. Limitations in the model, *i.e.* the truncation of the cluster expansion and the absence of coefficients describing stress or strain due to lattice constant mismatch, are responsible for the inaccuracies observed in Figure 4.

The model's predictive power was tested towards atomic swaps of the pure catalyst (Figure 4, top). The energetics of swapping atom positions are already reasonably well captured at the singly body level (blue points), where the energy of Pd and Ag only depends on the layer they are found in, which would be characteristic of a random alloy. The determination coefficient can, however, be further improved (from 0.76 to 0.82) by including two body terms. These corrective terms are found to be rather small ( $< 0.1$  eV). Therefore, extending the alloy description to computationally significantly more costly three body terms does not seem necessary and we adopt the model with two-body terms only, which gives a standard error of 0.14 eV for our simulations.

Regarding the adsorption energies of a single acetylene molecule on a p(3x3) cell (Figure 4, middle), the simplified triangular sites capture the overall tendency well (determination coefficient of 0.93). However, the straight "lines" formed by the blue dots demonstrate that the triangles fail to provide a realistic picture of the variations of adsorption energies as a function of the surface composition. Therefore, we have included an extended environment in the cluster expansion at the single molecule adsorption level. The additional six sites allow to increase the determination coefficient

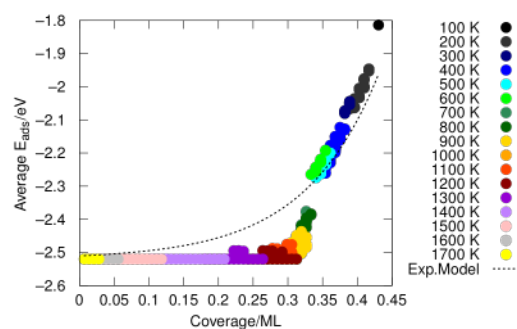


Figure 5. Average adsorption energy per acetylene molecule on Pd(111) as a function of the coverage, as obtained from simulations at 1 bar and varying the temperature. The dotted line indicates the exponential model proposed in ref 16.

to 0.96 and to lower the standard error from 0.19 to 0.14 eV. This demonstrates that the adsorption of acetylene on PdAg alloy surfaces is more complex to describe than previously thought, *i.e.*, that more than only three atoms are required to capture the full spectrum of adsorption energies on the alloy surface.

Finally, the bottom graph of Figure 4 shows the parity plot for the lateral interactions. The absolute values of the lateral interactions are very high (up to 8 eV), since it corresponds 3-8 acetylene molecules interacting with each other on a p(4x4) unit cell. Note, that all these systems have been fully optimized to the nearest local minimum, starting either from manually constructed systems or from structures reconstructed based on simulations on a p(4x4) cell using our Monte Carlo code. A large spread is observed within these configurations, with an  $R^2$  of 0.94 and a standard error of 0.54 eV. Indeed, the parameters for the lateral interactions are associated with the largest uncertainty (see Table S3). To analyze the lateral interactions, we have first considered the obtained parameters: Lateral interactions are generally strongly repulsive ( $\sim 0.8$  eV for third and  $\sim 1.2$  eV for second nearest neighbours), with the modulation between different terms being in line with expectations based on steric repulsion and unfavourable sharing of metallic sites. There is one exception, though: the Ag variant of third nearest neighbour interaction turns out to be slightly attractive (-0.3 eV). Test simulations with the specific term set to a slightly positive value (within the 95% uncertainty range of this parameter, see SI) are in full agreement with the conclusions drawn based on the mean parameters from the least squares fit. Second, Figure 5 compares the results from our simulations for pure Pd(111) with the mean field model proposed in our previous work. As can be seen, the simulations up to about 500 K probe

coverages larger than 0.3 ML and lower than 0.45 ML, a region in which the model prediction and the simulated data are in quite good agreement. Even at 100 K, higher coverages are prohibited by steric repulsion. The absence of long-ranged repulsive terms mostly affects the agreement between the model Hamiltonian and the continuum model between 0.2 and 0.3 ML, a region which is relevant only at temperatures well above 500 K. Therefore, our model is quite accurate in the realistic region of coverages. Since the lateral interactions are not determined very precisely but could be potentially very important (*vide infra*), we have performed additional sets of simulations that probe the influence of the precise value of these terms on the results (see SI). These simulations show that the observed results are overall robust with respect to such variations.

### Results and Discussion

Numerical experiments were designed bearing two goals in mind, namely 1) to predict the equilibrium distribution of Ag through the model, with special focus on the topmost layer, and 2) to assess the effect of the temperature on this distribution. To this end, the global molar fraction of Ag and the temperature were used as control parameters, keeping the simulated pressure of acetylene at the constant value of 1 bar. The fraction of Ag was scanned with steps of 0.1 or finer in regions with quickly changing properties. The temperature was scanned between 100 K and 1700 K, while the catalytically relevant temperature is between 300 and 400 K. Note that the simulations of temperatures above 500 K are of little practical relevance but shed light on the physics of the system (order-disorder transition). The simulated systems consisted of 576 metallic atoms distributed through the 4-layers model, with 288 hollow sites

available for adsorption. The configurational energy starts to fluctuate around its final value after about 10'000 steps (see Figure S1). All simulations were carried out to reach a total of 100'000 steps, with the last 90'000 steps, sampled every 100 steps, being used for analysis.

Figure 6 shows segregation profiles of the model, i.e. the fractional amount of Ag in the topmost layer as a function of the total Ag fraction. The straight dotted line, corresponding to an ideal model in which Ag and Pd are randomly placed into the surface is included as a guide to the eye. As long as the temperature is low enough, 100 K – 600 K, the profile of the Ag layer fraction lies well below the random distribution line, i.e., the surface is Pd rich. At catalysis temperature, the surface Pd fraction can be up to ~4 times higher than that in the bulk. At 900 K, the profile intersects the ideal distribution at 0.75 and its curvature changes; this trend continues at higher temperatures. At temperatures below 900 K, the simulations corresponding to total Ag molar fractions between 0.75 and 0.8 exhibit significant fluctuations, indicating that two arrangements are in competition (*vide infra*). Since the acetylene coverage drops with increasing temperature, starting from 1300 K, the surface is Ag rich for all molar fractions, in agreement with expectations based on the lower surface energy of Ag compared to Pd.

In summary, the segregation profiles show two regimes: at low (high) temperature and high (low) acetylene coverage, a Pd and Ag enrichment is obtained, respectively. Indeed, at low temperatures, acetylene adsorption is stable enough to attract a large fraction of Pd atoms from the subsurface to the topmost layer. As the temperature increases, thermal effects interfere with adsorption and Ag atoms tend to populate the surface as a result of their more favorable segregation energy and the increased importance of configurational entropy in the alloy. It is interesting to note that above 800 K the segregation profiles start to cross the random distribution. In other words, while at low Ag fraction

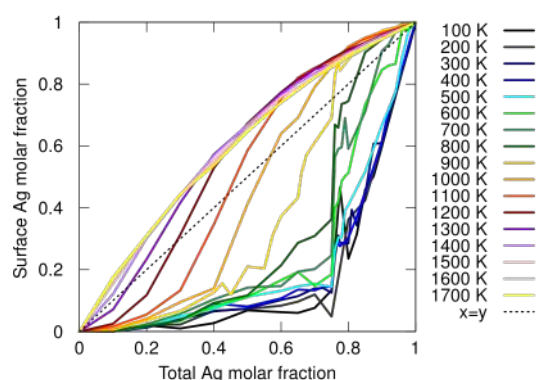


Figure 6. Segregation of the surface model as a function of the temperature.



Pd still segregates to the surface, the high temperature induces an increasingly large range of Ag fractions corresponding to a Ag rich surface. However, since the transition temperature for this mixed behavior is very high (above 800 K), it is not important for technologically relevant applications, such as membrane science or catalysis. In conclusion, acetylene severely modulates the surface composition, leading to a reverse segregation compared to vacuum conditions.

As mentioned in the Introduction, acetylene binds to more than one surface atom. One is then naturally led to assess the effect of this multi-dentate adsorption on the ordering of the topmost layer, i.e., island formation. In order to separate the vertical segregation from the “horizontal” in-plane ordering, Figure 7 top shows the populations of ensembles at different temperatures as a function of the Ag fraction in the topmost layer and compares it to random distributions. The bottom panel provides the acetylene coverage of these ensembles. Note that the saturation coverage obtained on Pd(111) agrees well with the measured value (1/3 ML), hence validating the accuracy of the model.<sup>35,36</sup> In fig. 7 top panel, overall, the points stay rather close to the random distributions: acetylene is not capable of strongly reorganizing the layer laterally even at low temperatures. This contrasts with our previous assessment based on a continuum model that showed marked deviations from random distributions upon acetylene adsorption.<sup>17</sup> Since the simulation at 100 K yields very similar distributions as at 300 K, the effect of entropy does not seem to be a determining factor for the in-plane (dis)ordering. However, in contrast to the results of the continuum model, Pd<sub>2</sub>Ag ensembles are also covered by acetylene at 300 K (see Figure 7 bottom). This is due to two effects. First, Figure 4 (middle) shows that the horizontal line of blue dots around -1.5 eV, which corresponds to adsorption on Pd<sub>2</sub>Ag, can go down to adsorption energies as low as -1.8 eV *depending on the environment*, while the adsorption energy on a Pd<sub>3</sub> ensemble can be as high as -1.6 eV if embedded in silver. In other words, the environment leads to a large distribution of binding energies that are overlapping between Pd<sub>3</sub> and Pd<sub>2</sub>Ag ensembles, counteracting the intrinsic island formation preference. Furthermore, even on Pd<sub>3</sub> only a bit more than one third of the triangular ensembles is occupied at 300 K (see Figure 7, bottom), which reduces the drive for island formation even more: in the continuum model, the mixed ensembles acted as inactive spacers, which allowed to maximize the coverage on Pd<sub>3</sub> ensembles. However, in the real space model

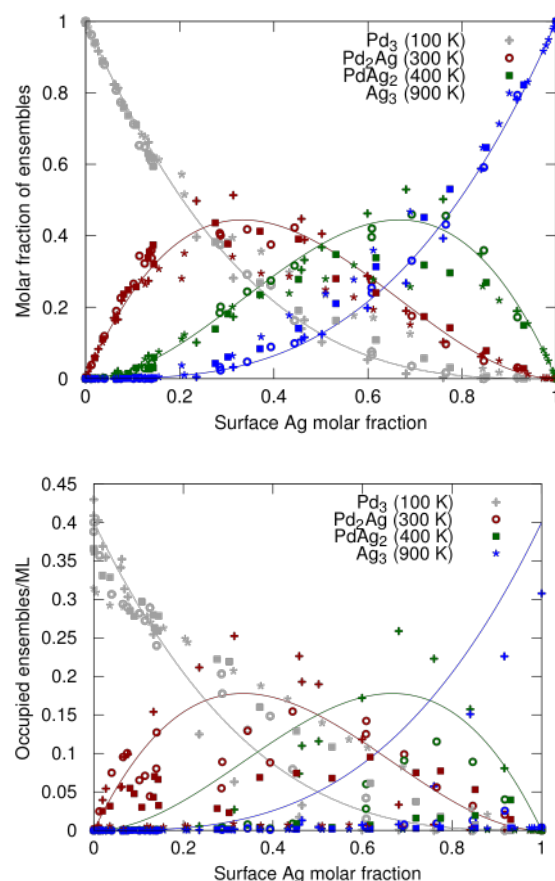


Figure 7. Surface ensemble populations (top, Pd<sub>3</sub> gray, Pd<sub>2</sub>Ag red, PdAg<sub>2</sub> green and Ag<sub>3</sub> blue) and their acetylene coverage (bottom) at 100 K (crosses), 300 K (circles), 400 K (squares), 900 K (stars) and random distribution (full lines) as a function of the surface layer Ag molar fraction.

presented herein, islands of Pd<sub>3</sub> are only covered by up to 0.4 ML and the mixed sites can still be occupied. Together, this correlation between occupied and unoccupied sites strongly reduces the island formation tendency. The intrinsic island formation tendency can be estimated by a back on the envelope calculation: The transformation of 2 Pd<sub>3</sub> and 1 Ag<sub>3</sub> ensembles into 3 Pd<sub>2</sub>Ag ensembles has only a relatively small effect ( $\{3x-1.5\} - \{2x-2.1\}$ ) eV = -0.3 eV). The small energetic difference rationalizes that the intrinsic ordering tendency of the system is not dominating if entropy and realistic lateral interactions are taken into account.

In Figure 7, we also present data for 400 and 900 K. These temperatures illustrate that the Pd<sub>3</sub> ensembles become more important with an increase in temperature: adsorption on PdAg<sub>2</sub> drops to zero at 400 K (green squares) and at 900 K also Pd<sub>2</sub>Ag (red crosses) is empty. Hence, we see a relative increase in the population of Pd<sub>3</sub> sites at surface Ag molar fractions larger than 0.5 with respect to lower temperatures, deviating from random distribution.

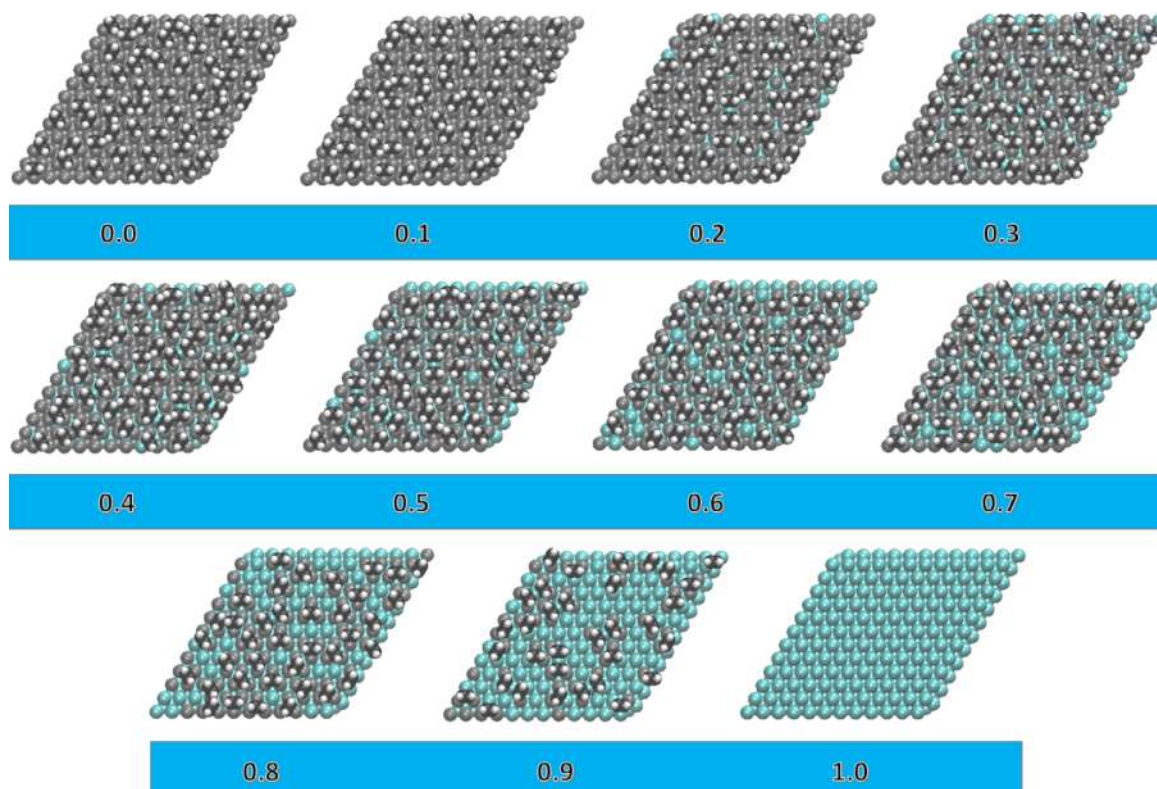


Figure 8. Snapshots of last accepted configuration at 300 K as a function of total Ag molar fraction.

The sensitivity of our results to the lateral interactions is shown in the SI. While the overall conclusions are not affected by the strength of the lateral interactions, more repulsive lateral interactions reduce the coverage of the mixed ensembles significantly.

The rapid change occurring at 0.7 – 0.8 Ag molar fraction is characteristic of the system and holds for all temperatures below 1000 K. Above 1000 K Ag surface segregation is dominating, suppressing phase transitions. Given that we are modelling a four layer system, the rapid change is suspiciously close to the composition where a full Pd layer cannot be formed anymore. However, according to Figure 7, the near random distributions are maintained over most Ag fractions. Nevertheless, the surface Ag content “jumps” from  $<0.2$  to  $>0.3$  for moderate temperatures, indicating a phase transition. It might be no coincidence that it is in this region where the random distributions of  $\text{Pd}_3$  and  $\text{Pd}_2\text{Ag}$  cross (0.25). In other words, the system changes from being dominated by (covered)  $\text{Pd}_3$  ensembles to a very disordered system where the coverage of  $\text{Pd}_3$  and  $\text{Pd}_2\text{Ag}$  ensemble is of similar magnitude.

Figure 8 depicts snapshots of the last accepted configuration at 300 K as a function of the total Ag content. The first observation is that the

acetylene overlayer is quite disordered. Second, despite the general impression gained from Figure 7 that many  $\text{Pd}_3$  ensembles remain empty, Figure 8 clarifies that for surfaces with a significant Ag content ( $>0.7$ ) almost all the Pd atoms are involved in binding acetylene, which contrasts with the Ag atoms which are frequently observed to act as inactive spacers between the Pd rich ensembles, in agreement with intuition. This also contributes to the overall low driving force towards island formation: in a Pd island (just like on pure Pd), Pd atoms are sometimes “wasted” to lower the steric repulsion, i.e., the lateral interactions. At high temperatures, a partial ordering in the surface layer is obtained: The  $\text{PdAg}_2$  sites being unoccupied, only the  $\text{Pd}_3$  ensembles contribute to the enthalpic stabilization of the system and they tend to organize into small islands or strips (not shown). Therefore, we have the untypical situation where higher temperatures lead to more ordered surfaces than lower temperatures, which follow the random distributions more closely.

## Conclusions

In this work, we have established a detailed model Hamiltonian for the Pd-Ag alloy configurations and for the acetylene adsorption on this alloy. We show that the adsorption energy of acetylene depends not only on the nature of the

triangular site on which it is bound, but also on the extended environment, i.e., the 9 nearest metallic atoms. Using the simple triangular sites does not provide an accurate description of the adsorption energy as a function of surface composition. The 24 interaction energy parameters have been fitted to roughly 400 DFT energies and provide overall an RMSD in the range of 0.2 eV. Lateral interactions are generally strongly repulsive and play a central role to determine the surface structure.

By performing Monte Carlo simulations based on this model Hamiltonian we demonstrate that, at realistic pressures, acetylene adsorption strongly modifies the composition of the Pd-Ag topmost layers in a wide range of operational conditions (300 K – 500 K). Reverse segregation pushes Pd atoms to populate the catalyst surface almost completely. This strong vertical reorganization of the alloy upon acetylene adsorption contrasts with the very moderate changes in the lateral organization (at a given surface concentration). Around an Ag fraction of 0.8 Ag a phase transition is observed for temperatures below 1000 K. Above this transition point, the alloy surface is no longer dominated by Pd<sub>3</sub> ensembles. Since the Pd-Ag surface sticks closely to random distributions, at low enough temperatures (< 400 K) and high total Ag fractions (>0.8), a majority of acetylene molecules can be adsorbed on Pd<sub>2</sub>Ag ensembles.

This thermodynamic vertical reorganization of the alloy surface under a pressure of acetylene is likely to be involved in the experimentally observed aging process of AgPd selective hydrogenation catalysts. In other words, since acetylene induces reverse segregation, the ideal selective hydrogenation catalyst with well dispersed Pd ensembles, surrounded by Ag, is thermodynamically unstable. However, if the ideal catalyst can be prepared and the temperature is kept low in order to reduce the diffusion process leading to the surface re-ordering, the catalyst lifespan is likely to be increased. Similarly, structural agents, be it third metals, supports or ligands, that would slow down diffusion and/or counteract the effect of acetylene would increase the stability of the active catalyst.

### Supporting Information available

Cluster expansion parameters, additional Figures and all geometries are provided. All programs for numerical simulations are also available.

### Corresponding Author

Stephan.steinmann@ens-lyon.fr; sautet@ucla.edu

### Acknowledgements

*Ab initio* calculations were performed using the local HPC resources of PSMN at ENS-Lyon. This work was granted access to the HPC resources of CINES and IDRIS under the allocation 2014-080609 made by GENCI. *Selective Hydrogenation of Acetylene in an Ethylene-Rich Flow: Insights from Molecular Modeling* is a research project funded by TOTAL Refining & Chemicals and the ANRT.

### References

- (1) Callister, W. D.; Rethwisch, D. G. *Materials Science and Engineering. An Introduction*, 7th ed.; Wiley Publishers: New York, 2006.
- (2) Tsai, M.-H.; Yeh, J.-W. High-Entropy Alloys: A Critical Review. *Mater. Res. Lett.* **2014**, 2 (3), 107–123.
- (3) Zou, Y.; Ma, H.; Spolenak, R. Ultrastrong Ductile and Stable High-Entropy Alloys at Small Scales. *Nat. Commun.* **2015**, 6, 7748.
- (4) Dowben, P. A.; Miller, A. *Surface Segregation Phenomena*; CRC Press: Boca Raton (FL), 1990.
- (5) De Clercq, A.; Giorgio, S.; Mottet, C. Pd Surface and Pt Subsurface Segregation in Pt<sub>1</sub>-cPd<sub>c</sub> Nanoalloys. *J. Phys. Condens. Matter* **2016**, 28, 64006.
- (6) Clarke, J. K. A. Selectivity in Catalysis by Alloys. *Chem. Rev.* **1975**, 75 (1), 291–305.
- (7) Tao, F.; Salmeron, M. In Situ Studies of Chemistry and Structure of Materials in Reactive Environments. *Science* **2011**, 331 (6014), 171–174.
- (8) Hirschl, R.; Delbecq, F.; Sautet, P.; Hafner, J. Adsorption of Unsaturated Aldehydes on the (111) Surface of a Pt-Fe Alloy Catalyst from First Principles. *J. Catal.* **2003**, 217, 354–366.
- (9) Zhu, B.; Creuze, J.; Mottet, C.; Legrand, B.; Guesmi, H. CO Adsorption-Induced Surface Segregation and Formation of Pd Chains on AuPd(100) Alloy: Density Functional Theory Based Ising Model and Monte Carlo Simulations. *J. Phys. Chem. C* **2016**, 120 (1), 350–359.
- (10) Chen, W.; Schmidt, D.; Schneider, W. F.; Wolverton, C. Ordering and Oxygen

- Adsorption in Au/Pt(111) Surface Alloys. *J. Phys. Chem. C* **2011**, *115*, 17915–17924.
- (11) Lovvik, O. M.; Opalka, S. M. Reversed Surface Segregation in Palladium-Silver Alloys due to Hydrogen Adsorption. *Surf. Sci.* **2008**, *602*, 2840–2844.
- (12) Svenum, I. H.; Herron, J. A.; Mavrikakis, M.; Venvik, H. J. Adsorbate-Induced Segregation in a PdAg Membrane Model System: Pd<sub>3</sub>Ag(1 1 1). *Catal. Today* **2012**, *193* (1), 111–119.
- (13) Padama, A. A. B.; Kasai, H.; Budhi, Y. W. Hydrogen Absorption and Hydrogen-Induced Reverse Segregation in Palladium-Silver Surface. *Int. J. Hydrogen Energy* **2013**, *38* (34), 14715–14724.
- (14) Vignola, E.; Steinmann, S. N.; Al Farra, A.; Vandegehuchte, B. D.; Curulla, D.; Sautet, P. Evaluating the Risk of C–C Bond Formation during Selective Hydrogenation of Acetylene on Palladium. *ACS Catal.* **2018**, *8*, 1662–1671.
- (15) Ponc, V.; Bond, G. C. *Catalysis by Metals and Alloys*; Elsevier: Amsterdam, 1995.
- (16) Engstfeld, A. K.; Hoster, H. E.; Behm, R. J. Formation, Atomic Distribution and Mixing Energy in Two-Dimensional Pd<sub>x</sub>Ag<sub>1-x</sub> Surface Alloys on Pd(111). *Phys. Chem. Chem. Phys.* **2012**, *14* (30), 10754.
- (17) Vignola, E.; Steinmann, S. N.; Vandegehuchte, B. D.; Curulla, D.; Sautet, P. C<sub>2</sub>H<sub>2</sub>-Induced Surface Restructuring of Pd-Ag Catalysts: Insights from Theoretical Modeling. *J. Phys. Chem. C* **2016**, *120*, 26320–26327.
- (18) Blochl, P. E. Projector Augmented-Wave Method. *Phys. Rev. B* **1994**, *50* (24), 17953–17979.
- (19) Kresse, G.; Joubert, D. From Ultrasoft Pseudopotentials to the Projector Augmented-Wave Method. *Phys. Rev. B* **1999**, *59* (3), 1758–1775.
- (20) Kresse, G.; Hafner, J. Ab Initio Molecular Dynamics for Liquid Metals. *Phys. Rev. B* **1993**, *47* (1), 558–561.
- (21) Kresse, G.; Furthmüller, J. Efficient Iterative Schemes for Ab Initio Total-Energy Calculations Using a Plane-Wave Basis Set. *Phys. Rev. B* **1996**, *54* (16), 11169–11186.
- (22) Perdew, J. P.; Burke, K.; Ernzerhof, M. Generalized Gradient Approximation Made Simple. *Phys. Rev. Lett.* **1996**, *77*, 3865–3868.
- (23) Steinmann, S. N.; Corminboeuf, C. Comprehensive Benchmarking of a Density-Dependent Dispersion Correction. *J. Chem. Theory Comput.* **2011**, *7*, 3567–3577.
- (24) Pack, J. D.; Monkhorst, H. J. Special Points for Brillouin-Zone Integrations. *Phys. Rev. B* **1976**, *13* (12), 5188–5192.
- (25) Methfessel, M.; Paxton, A. T. High-Precision Sampling for Brillouin-Zone Integration in Metals. *Phys. Rev. B* **1989**, *40* (6), 3616–3621.
- (26) Frenkel, D.; Smit, B. *Understanding Molecular Simulations*; Academic Press: San Diego, 1996.
- (27) Hill, T. L. *An Introduction to Statistical Thermodynamics*; Dover Publications, Ed.; New York, 1960.
- (28) Sanchez, J. M.; Ducastelle, F.; Gratias, D. Generalized Cluster Description of Multicomponent Systems. *Phys. A Stat. Mech. its Appl.* **1984**, *128* (1–2), 334–350.
- (29) Lee, T. D.; Yang, C. N. Statistical Theory of Equations of State and Phase Transitions. II. Lattice Gas and Ising Model. *Phys. Rev.* **1952**, *87* (3), 410–419.
- (30) Ruban, A. V.; Abrikosov, I. A. Configurational Thermodynamics of Alloys from First Principles: Effective Cluster Interactions. *Reports Prog. Phys.* **2008**, *71* (4), 46501.
- (31) Dunphy, J.; Rose, M.; Behler, S.; Ogletree, D.; Salmeron, M.; Sautet, P. Acetylene Structure and Dynamics on Pd(111). *Phys. Rev. B* **1998**, *57* (20), R12705–R12708.
- (32) Barata, J. C. A.; Hussein, M. S. The Moore–Penrose Pseudoinverse. A Tutorial Review of the Theory. *Brazilian J. Phys.* **2012**, *42* (146–165).
- (33) Bollen, K. A.; Jackman, R. W. Regression Diagnostics: An Expository Treatment of Outliers and Influential Cases. In *Modern Methods of Data Analysis*; Sage: Newbury Park, 1990; pp 257–291.
- (34) Bishop, C. M. *Pattern Recognition and*

*Machine Learning*; Springer-Verlag: New York, 2006.

- (35) Janssens, T. V. W.; Völkening, S.; Zambelli, T.; Winterlin, J. Direct Observation of Surface Reactions of Acetylene on Pd(111) with Scanning Tunneling Microscopy. *J. Phys. Chem. B* **1998**, *102* (34), 6521–6528.
- (36) Gates, J. A.; Kesmodel, L. L. Thermal Evolution of Acetylene and Ethylene on Pd(111). *Surf. Sci.* **1983**, *124* (1), 68–86.



# TOC Graphic

